

# Technical Reports

## Current Limits of X-ray Microdiffraction in Soft Condensed Matter Experiments

C. Riekel, M. Burghammer and S. Roth

European Synchrotron Radiation Facility, B.P. 220, F-38043 Grenoble Cedex, France

*Received 14th December 2001; accepted in revised form 16th April 2002.*

### Introduction.

The ID13 beamline is providing microbeams for wide-angle (WAXS) and small-angle (SAXS) X-ray scattering experiments. An appreciable fraction of experiments is performed in the area of synthetic and biopolymeric materials. In the following review an overview on existing instrumentation, its limitations and the ongoing refurbishment program is given.

### Generation of microbeams

The ID13 beamline is installed at a low- $\beta$  section [1]. The current radiation source is a 46mm period undulator (U46), which provides a large spectral tuning range. An 18mm period in-vacuum undulator (U18) will be installed in 2002 [2, 3]. Its fundamental will provide at 12.9 keV about a 7-fold flux increase as compared to U46. The optical system comprises a liquid N<sub>2</sub> cooled Si-111 double monochromator and a condensing (ellipsoidal) mirror (Fig.1). The photon source point of  $134_{\text{hor}} * 23_{\text{vert}}$   $\mu\text{m}$  fwhm (full-width at half maximum) is geometrically demagnified by a factor of 10 by the condensing mirror [4]. The observed focal spot of about  $20_{\text{hor}} * 40_{\text{vert}}$   $\mu\text{m}$  fwhm is, however, considerably larger than the expected  $13_{\text{hor}} * 2_{\text{vert}}$   $\mu\text{m}$  fwhm. This is mainly due to mirror slope errors of  $4.2_{\text{meridional}} * 12.6_{\text{tangential}}$   $\mu\text{rad}$  [5]. Smaller beam sizes at the sample position are defined by add-on optics such as a capillary, collimator or waveguide.

Currently available tapered capillaries provide about a 2  $\mu\text{m}$  fwb (full-width at base) spot with a divergence of 2.3 mrad at 13 keV. Capillaries are used for ultra-low background WAXS experiments but require a short (<0.5 mm) sample-to-capillary exit distance [6]. The divergence and shielding of the capillary exit limits low-angle applications in practice to  $Q_{\text{min}} \approx 0.4 \text{ nm}^{-1}$  ( $Q=4\pi \sin\Theta/\lambda$ ) [7].

Collimating optics based on Pt/Rh electron microscopy apertures permits a reduction of the minimum beam size to about 5  $\mu\text{m}$  fwhm. For a divergence of 0.2 mrad in the vertical plane one can reach  $Q_{\text{min}} \approx 0.06 \text{ nm}^{-1}$  by using an electron microscopy guard aperture. The horizontal divergence at the sample position of about 2.1 mrad can be further reduced by slits in front of the collimating system. On-going instrumental developments aim at reducing the beam size to about 2  $\mu\text{m}$  by apertures while maintaining the  $Q_{\text{min}}$  limit.

X-ray waveguide optics is used without the ellipsoidal condensing mirror and provides a coherent slab-like beam with  $\leq 100 \text{ nm}$  size in the vertical direction [8]. At 13 keV the TE<sub>0</sub>-mode has a divergence of about 1 mrad. Horizontal beam compression to about 3  $\mu\text{m}$  by a cylindrically bent multilayer mirror has been demonstrated [9]. It is expected that other hard x-ray optics, which provides a two-dimensional sub-mm spot (e.g. zone plates), will become available in the future.

The second experimental hutch, which is currently being refurbished with a Kirkpatrick-Baez (KB) mirror-system, will be used principally for scanning SAXS/WAXS applications (Fig.1) This KB-system is based on two cylindrically bent, 170 mm long mirrors [10]. Mirror slope errors of  $\leq 0.9 \mu\text{rad}$  fwhm are now technologically feasible [11]. Spot sizes expected from ray-tracing calculations assuming a 0.9  $\mu\text{rad}$  fwhm slope error are shown in Fig.1 [6]. These calculations do not, however, take beam instabilities due to the source and monochromator vibrations introduced by the liq. N<sub>2</sub> cooling system into account. A beam defining collimating system will therefore be used in order to obtain a stable beam at the sample position.

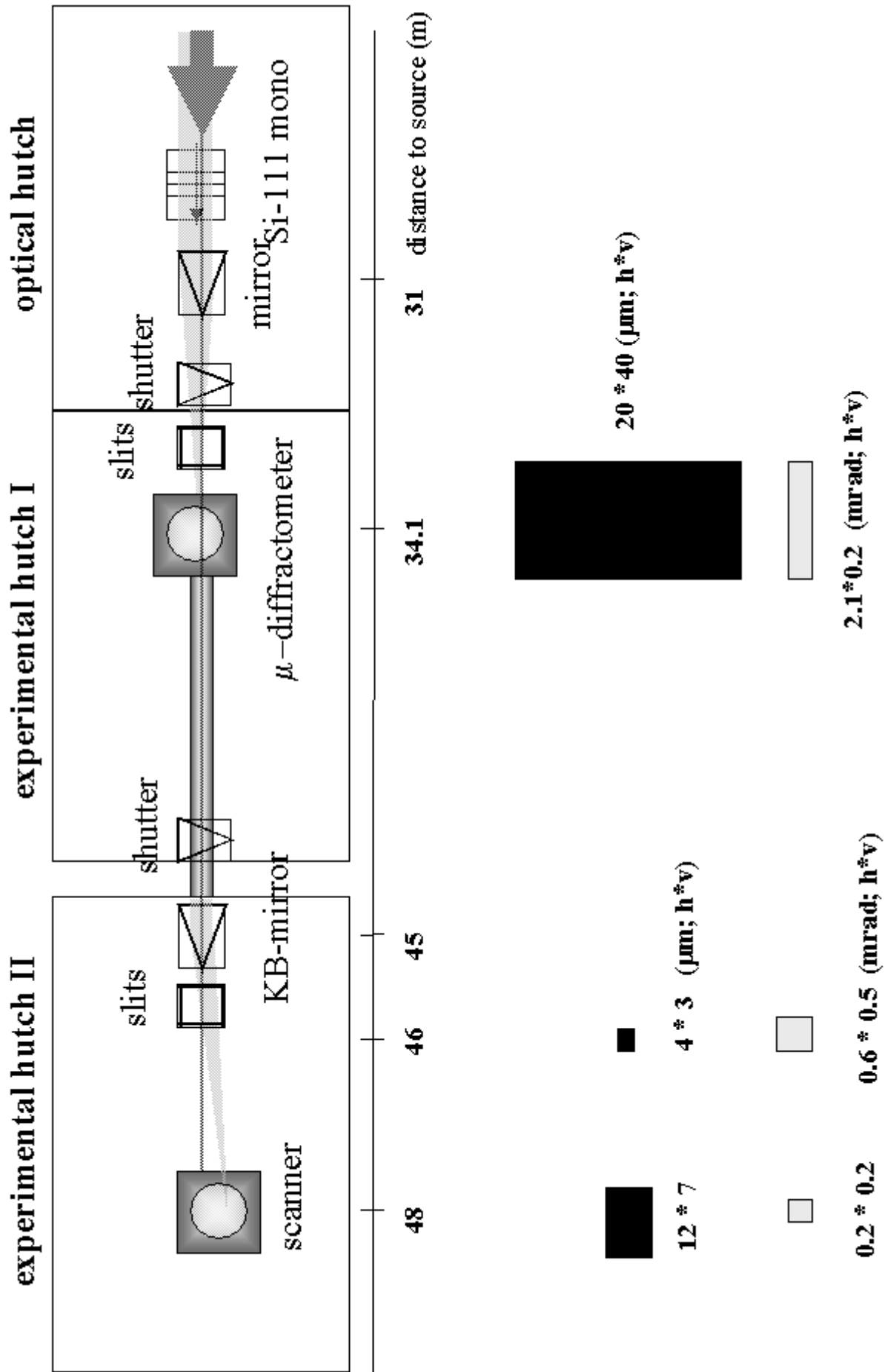


**Figure 1:** Schematic design of ESRF microfocus beamline (ID13). The size (experimental value) and divergence of the focal spot in the first experimental hutch as well as the calculated values in the second experimental hutch are indicated.

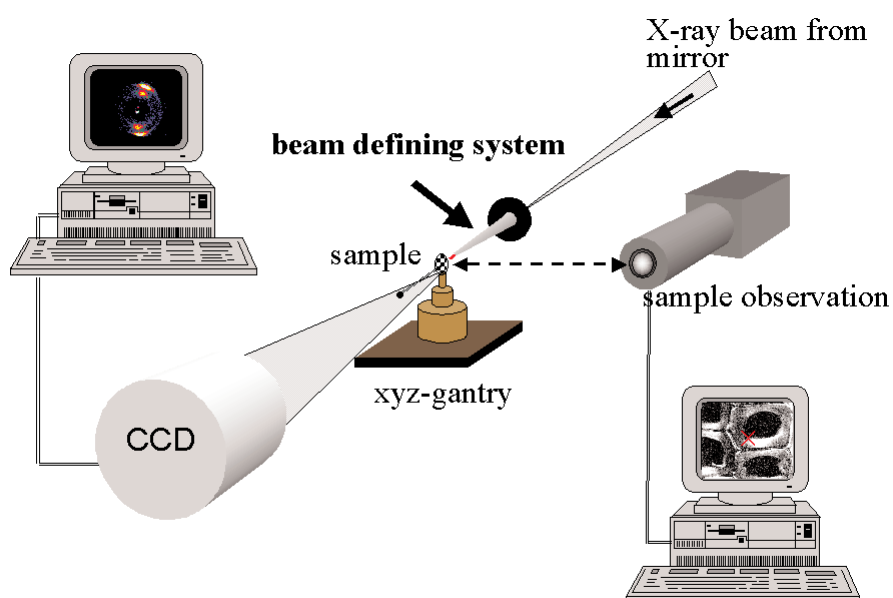


**Figure 2:** Schematic design of scanning setup [4]. The sample is pre-aligned with a video microscope and transferred into the beam via an x/y/z gantry.

## Sample environment

The range of microdiffraction applications has led to the development of different setups for scanning diffractometry and single crystal diffractometry [4]. These setups are currently used in the first experimental hutch and will be installed in separate hutches after the refurbishment [4].

The scanning setup is shown schematically in Fig.2. The distance x-ray beam-to-optical microscope is calibrated by a polymer fibre cross to about  $\pm 1$  mm. The scanning setup is principally used for experiments on extended samples and complex sample environments with beam sizes down to about 2  $\mu\text{m}$ . Sub-mm beams will require the development of a more precise positioning and sample observation system than currently available [9].

An interesting feature of the micro-collimating optics is that one can record SAXS and WAXS with the same detector provided its angular resolution at a given opening angle is sufficient [12]. This is the case for a 16-bit slow-scan MAR-CCD detector with a 130 mm diameter converter-screen and a point spread function of about 0.1 mm. At the level of a few mm beam size thermal drifts reduce the long-term stability of the collimating system which is currently composed of individually motorized apertures. This can be improved by controlling the temperature of the experimental hutch to  $\pm 0.5^\circ\text{C}$  but is not very practical for routine user operation. A more stable block collimating system incorporating

the apertures is therefore currently being developed.

The SAXS/WAXS pattern of a collagen fibre recorded with a 5  $\mu\text{m}$  beam at 13 keV demonstrates that the first order ( $d=65$  nm) can be resolved from the beamstop (Fig.3). Fig.4 shows SAXS/WAXS patterns of single fibres from the minor (*MI*) and major (*MA*) ampullate glands of a *Nephila senigalensis* spider recorded with a 10  $\mu\text{m}$  beam during an in-situ extrusion experiment [13]. The equatorial streak and the meridional 8nm peak in *MA*-silk suggest a fibrillar morphology composed of crystalline and amorphous domains [13, 14]. WAXS data show that the crystalline domains consist of poly(alanine) chains [15, 16]. The absence of a meridional 8 nm peak in *MI*-silk could be due to an increase in the size of the crystalline domains, which would shift the meridional peak to smaller Q-values. This is corroborated by *MI*-sequencing data showing larger alanine repeats as compared to *MA*-silk [17-19].

A limitation for scanning diffractometry is the exposure time of up to several seconds per frame (single pattern in a sequence) of slow-scan CCD cameras. This is not a problem for the collection of high-resolution fibre diffraction data which may take up to several minutes. If, however, data collection can be limited to a few statistically significant reflections (e.g. determination of Herman's orientation function [20]), then the framing rate should be matched to the frame exposure time. Framing rates of 5-10 Hz can be obtained with 12-

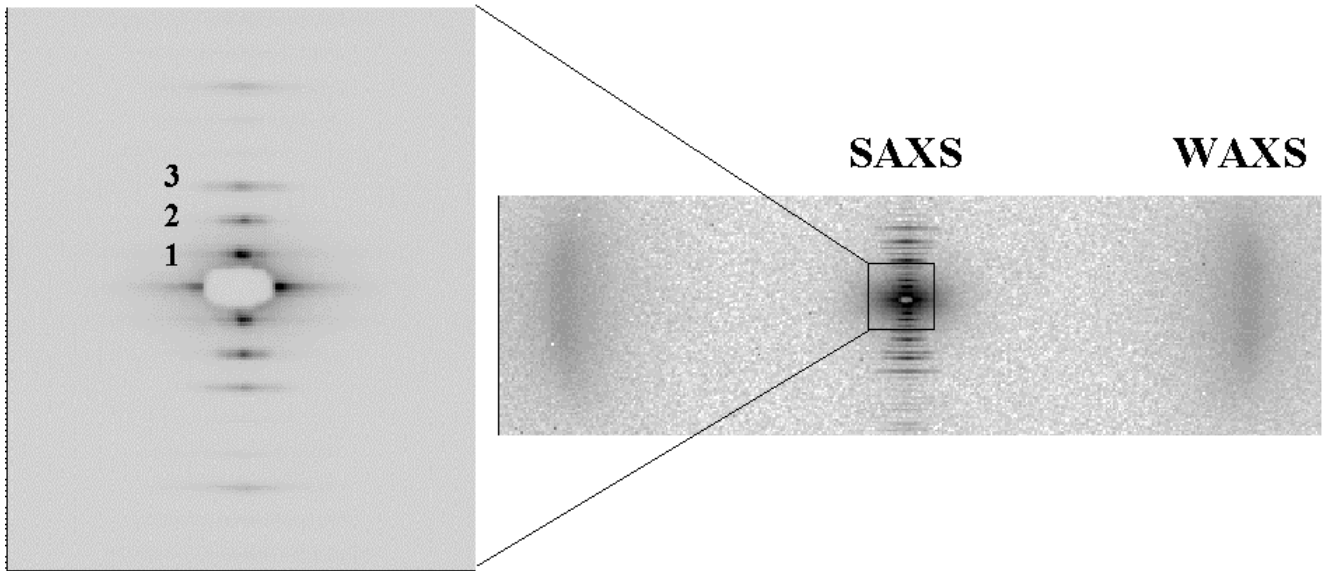


**Figure 3:** Combined SAXS/WAXS experiment for a dry rat's tail collagen fibre. The first order reflection (65 nm) is well separated from the beamstop.

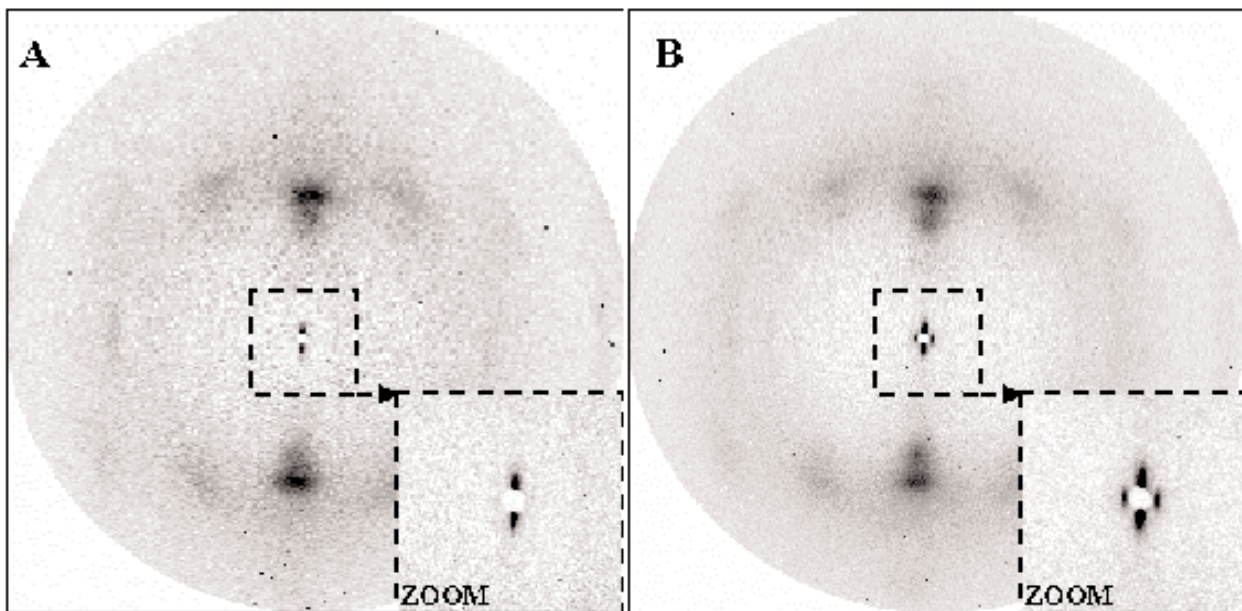


**Figure 4:** Combined SAXS/WAXS of minor and major ampullate *Nephila senigalensis* silk fibres during in-situ spinning [13]. The fibre axis is horizontally oriented. Note the difference in meridional scattering of the two fibres. The meridional major ampullate peak has a d spacing of about 8 nm. The edge of the beamstop defines  $Q_{min} \gg 0.6 \text{ nm}^{-1}$ .

14-bit image-intensified CCD detectors. Selective area readout allows further increasing the framing rate. Fig.5 shows the variation of the relative integrated intensity and relative azimuthal width of the (200) reflection of a 12  $\mu\text{m}$  diameter p(paraphenylene terephthalamide) fibre for three sub-second frame exposure times. Data were recorded with a 10Hz, 12 bit GemStar detector (Photonic Science). The data suggest that statistically significant profile parameters can be recorded for strong reflections at the 0.1 sec exposure level. The angular resolution at a given opening angle and

hence SAXS/WAXS capability of such systems is, however, currently more limited as compared to slow-scan systems. The quest for large-area detectors with high framing rate, high dynamic range, single photon counting capability and angular resolution is shared with biocrystallography. The pixel detector technology is an option for such applications [21]. Although fast framing detectors and the possibility for fast analysis of selected reflections [22] are becoming available, an integration in a dedicated scanning system will be required. This could for example allow determining Herman's orientation

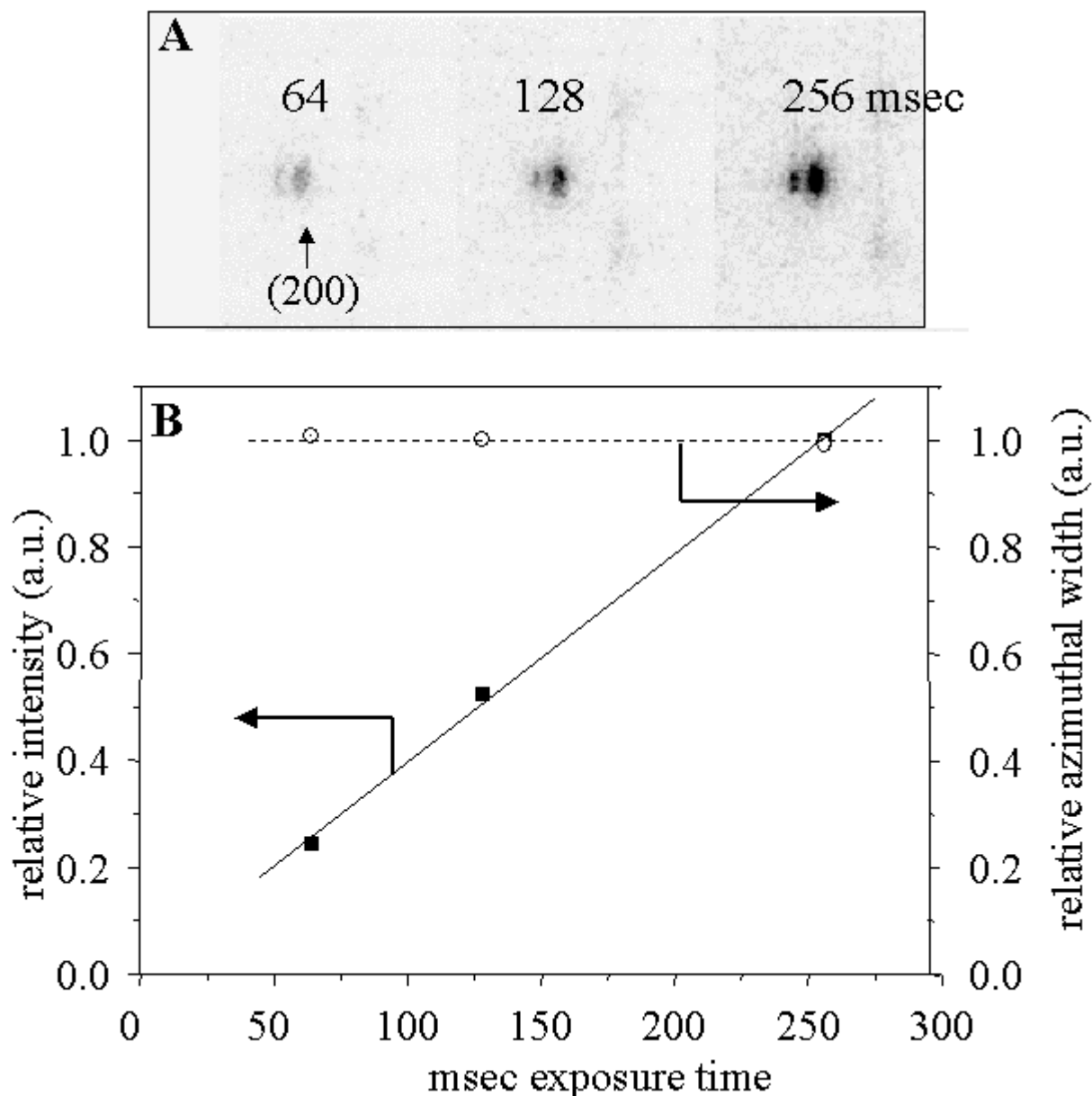


**Figure 5:** Single fibre diffraction for a 12 mm diameter PPTA-fibre recorded with a 12 bit image intensified CCD (Photonic Science). A: strongest equatorial reflections for three sub-second exposure times. B: relative integrated intensity and relative azimuthal width of (200) reflection.

function [20] for a fibre in "real time" during a stress/strain experiment.

Flux densities of  $\approx 108$  ph/s/ $\mu\text{m}^2/\text{mA}$  at the exit of a glass capillary allow recording WAXS patterns from an about  $1 \mu\text{m}$  thick *MI*-silk fibre [23]. Averaging of several frames recorded along the fibre axis was, however, necessary. SAXS/WAXS patterns of such fibres at a one position should become accessible with a further increase of flux densities due to the use of an in-vacuum undulator (see above) and more efficient focusing optics. Primary radiation damage (PRD) due to breaking of chemical bonds is the ultimate limit for diffraction experiments while secondary radiation damage (SRD) due to the propagation of PRD-products can be reduced by cryo-cooling techniques [24, 25]. Single photon

counting capability (see above) is important in particular for in-situ experiments where SRD plays a role.

Single fibre diffraction experiments can also be performed using a micro-diffractometer which has been developed for protein crystallography [26]. A  $5 \mu\text{m}$  beam and the possibility for on-axis observation of the sample is particularly useful for rapidly selecting specific points on a fibre or for examining a mixture of fibres. A He-filled tube can be used for low-angle applications down to  $Q_{\min} \approx 0.21 \text{ nm}^{-1}$  (Fig.6). Improvements in the collimating system will be required in order to reduce this value. It is expected that ongoing instrumental development will allow the combination of scanning features with on-line observation capabilities. Techniques for sample

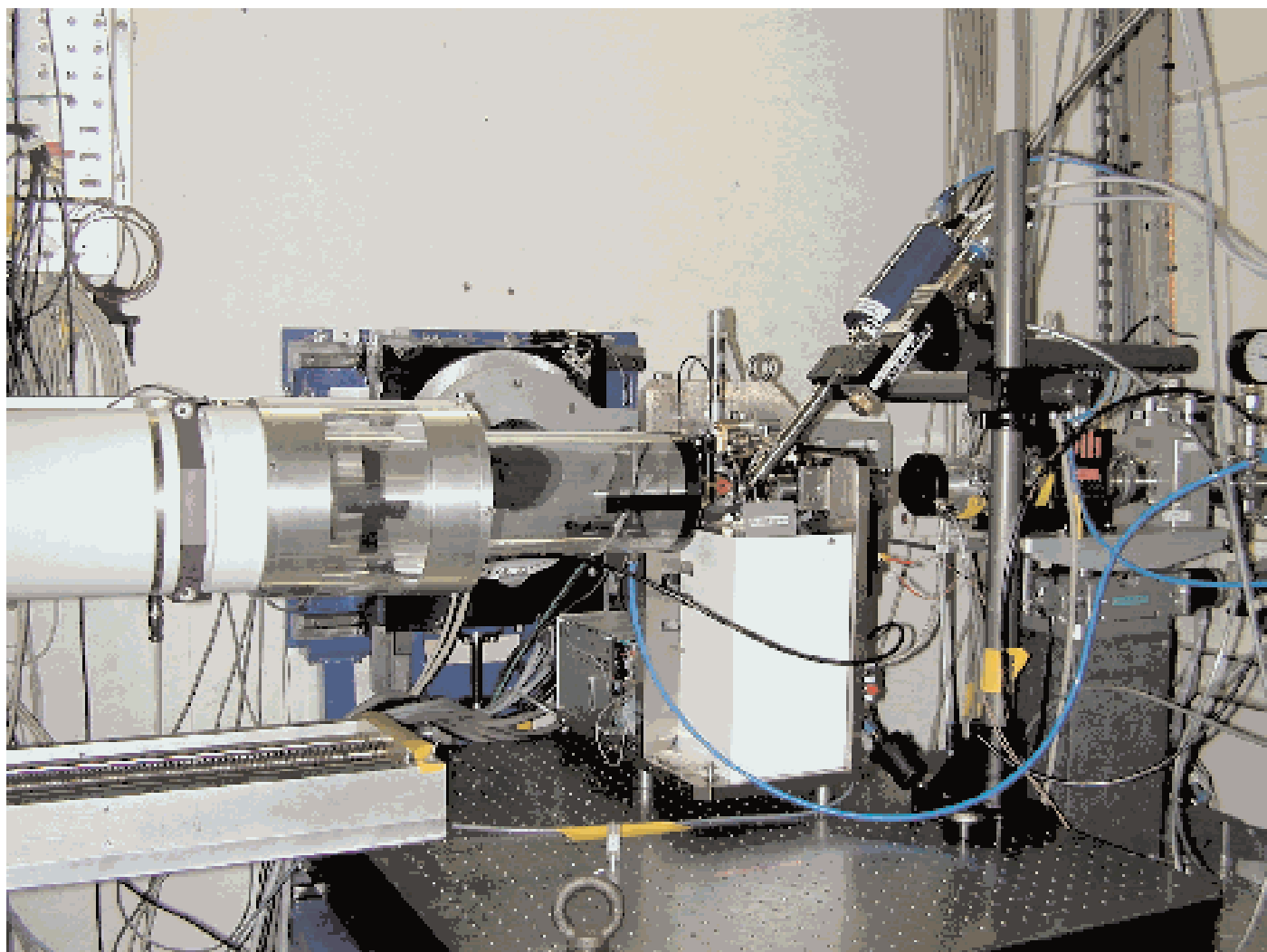


**Figure 6:** Microgoniometer with He-tube attached to CCD detector for low-angle applications.

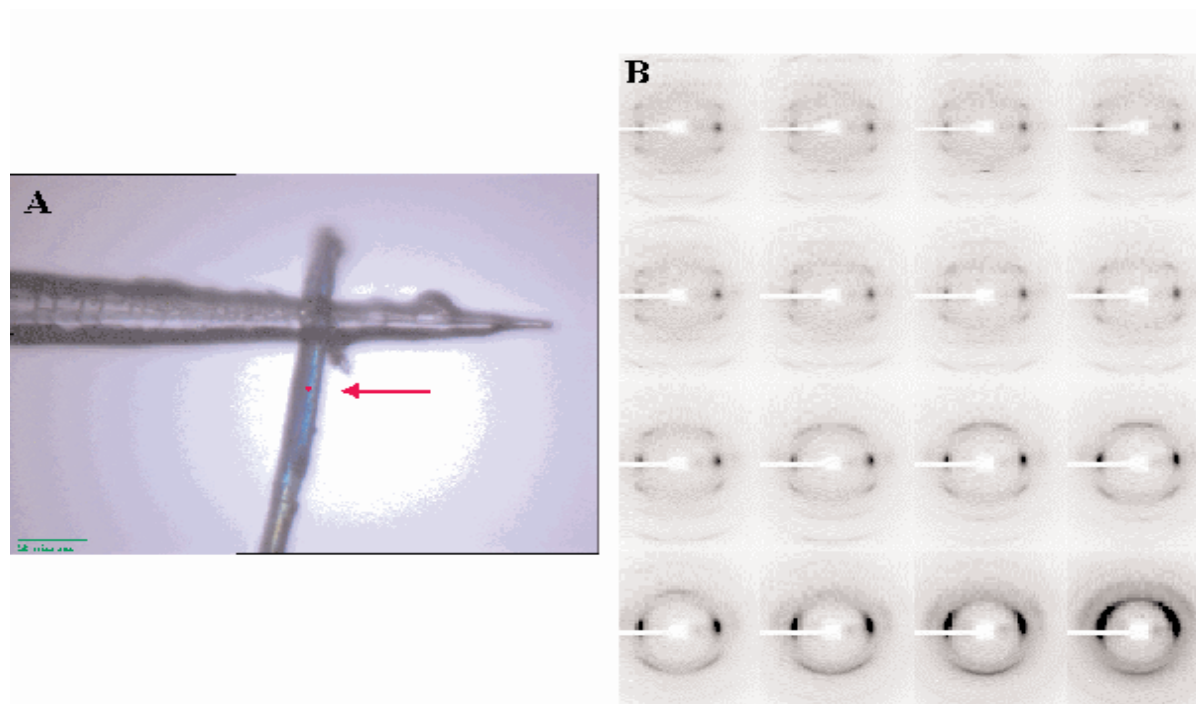


**Figure 7:** A: Optical image of Bombyx mori fibre glued to a glass capillary tip recorded on the microgoniometer. The red circle corresponds to a 5 mm diameter X-ray beam. B: WAXS frames recorded during the rotation of a Bombyx mori fibre around an axis normal to the fibre axis. Every rotational step was 50 with a recording time of 30 sec.

manipulation are similar to single microcrystal diffractometry. Thus an image of a short piece of *Bombyx mori* cocoon fibre glued to a glass tip prior to alignment is shown in Fig.7.a. Fig.7.b shows a sequence of frames recorded during the rotation of such a fibre around an axis normal to the fibre axis. Individual frames correspond to a 5° rotation within 30 sec. The beam is nearly orthogonal to the fibre axis in the first frame but nearly parallel in the last frame.

## Conclusions

The current generation of microbeams available at ID13 allows WAXS experiments on fibres down to about 1 mm diameter in exceptional cases [23]. The use of cryo-cooling techniques, higher flux densities by in-vacuum undulators, better polished mirrors and single photon counting detectors should make SAXS/WAXS experiments at this level become routinely available. Critical issues like long-term beam stability, intensity monitoring or absolute intensity scaling have to be addressed but there is no reason why these technical problems could not be resolved. On-going X-ray optical developments allow extending beam sizes to the 100 nm range [9]. This will pose new challenges to sample environment setups including sample observation.

## Acknowledgements

The development of the microbeam setup at ID13 is a team effort. We would like to mention in particular the contributions of P. Engström (Göteborg) and M. Müller (Kiel). The microgoniometer has been developed as a common project between EMBL-Grenoble and ESRF. We wish to thank in particular S. Cusack and F. Cipriani (EMBL) for their collaboration. The ESRF optics group (O. Hignette et al. has developed the KB-system.

## References

[1] [http://www.esrf.fr/exp\\_facilities/ID13/index.html](http://www.esrf.fr/exp_facilities/ID13/index.html).

[2] VanVaerenbergh, P., J. Chavanne, and P. Elleaume. Recent Developments of Insertion Devices at the ESRF. in *1999 Particle Accelerator Conference*. 1999. New York.

[3] Chavanne, J., P. Elleaume, and P. VanVaerenbergh, In-Vacuum Undulators. *ESRF*

*Newsletter*, 2000. **34**: p. 29-31.

- [4] Riekkel, C., New Avenues in X-ray microbeam experiments. *Rep. Prog. Phys.*, 2000. **63**: p. 233-262.
- [5] Riekkel, C., P. Bösecke, and M.S.d. Rio, Two High Brilliance Beamlines at the ESRF for Microfocus. *Rev. Sci. Instrum.*, 1992. **63**(1): p. 974-981.
- [6] Riekkel, C. and L. Vincze, *Status and Perspectives of Capillary Optics at a 3rd Generation Synchrotron Radiation Source*. in press, 2002.
- [7] Engström, P. and C. Riekkel, Low-Angle Synchrotron Radiation Diffraction with Glass Capillary Optics. *J. Synchr. Rad.*, 1996. **3**: p. 97-100.
- [8] Jark, W., et al., Submicrometer beamsizes observed at the exit of an x-ray waveguide. *J. of Appl. Phys.*, 1996. **80**(9): p. 4831-4836.
- [9] Müller, M., et al., Microcrystallography with an X-ray waveguide. *J. Appl. Cryst.*, 2000. **33**: p. 1231-1240.
- [10] Hignette, O., et al. Submicron focusing of hard X-rays with reflecting surfaces at the ESRF. in *SPIE Conference Proceedings* 4499. 2001. San Diego.
- [11] Hignette, O., et al. Towards the preparation of optical surfaces preserving the coherence of hard X-rays. in X-ray mirrors, crystals and multilayers II. 2001: *SPIE Conference Proceedings*.
- [12] Riekkel, C., M. Burghammer, and M. Müller, Microbeam Small-Angle Scattering Experiments and their Combination with Microdiffraction. *J. Appl. Cryst.*, 2000. **33**: p. 421-423.
- [13] Riekkel, C. and F. Vollrath, Spider silk fibre extrusion: combined wide- and small-angle X-ray microdiffraction experiments. *Int. J. Biol. Macrom.*, 2001. **29**(3): p. 203-210.
- [14] Yang, Z., D.T. Grubb, and L.W. Jelinski, Small-Angle X-ray Scattering of Spider Dragline Silk.

- Macromolecules*, 1997. **30**: p. 8254 - 8261.
- [15] Grubb, D.T. and L.W. Jelinski, Fiber Morphology of Spider Silk: The Effects of Tensile Deformation. *Macromolecules*, 1997. **30**(10): p. 2860-2867.
- [16] Bram, A., *et al.*, X-ray diffraction from single fibres of spider silk. *Journal of applied crystallography*, 1997. **30**(Pt3): p. 390-392.
- [17] Guerette, P., *et al.*, The spider silk fibroin gene family: gland specific expression controls silk properties. *Science*, 1996. **272**(5258): p. 112-115.
- [18] Colgin, M.A. and R. Lewis, Spider minor ampullate silk proteins contain new repetitive sequences and highly conserved non-silk-like "spacer regions". *Protein Sci.*, 1998. **7**: p. 667-672.
- [19] Gosline, J.M., *et al.*, The mechanical design of spider silks: from fibroin sequence to mechanical function. *J. of Exp. Biol.*, 1999. **202**: p. 3295-3303.
- [20] Stein, R.S. and G.L. Wilkes, *Physico-Chemical Approaches to the Measurement of Anisotropy, in Structure and Properties of Oriented Polymers*, I.I. Ward, Editor. 1975, Applied Science Published Ltd: London. p. 57-145.
- [21] Brönnimann, C., *et al.*, [http://pc2462.psi.ch/pix\\_gen.html](http://pc2462.psi.ch/pix_gen.html).
- [22] Riekkel, C., *et al.*, An X-ray Microdiffraction Study of Chain-Orientation in Poly(p-phenylene terephthalamide). *Macromolecules*, 1999. **32**: p. 7859-7865.
- [23] Riekkel, C., *et al.*, Microstructural homogeneity of support silk spun by *Eriophora fuliginea* (C.L. Koch) determined by scanning X-ray microdiffraction. *Naturwissenschaften*, 2001. **88**: p. 67-72.
- [24] Henderson, R., Cryo-protection of protein crystals against radiation damage in electron and X-ray diffraction. *Proc. Roy. Soc. B*, 1990. **241**: p. 6-8.
- [25] Teng, T. and K. Moffat, Primary radiation damage of protein crystals by intense synchrotron X-ray beam. *J. Synchrotron Rad.*, 2000. **7**: p. 313-317.
- [26] Perrakis, A., *et al.*, Protein microcrystals and the design of a diffractometer: current experience and plans at EMBL and ESRF/ID13. *Acta Cryst.*, 1999. **D55**: p. 1765-1770.